Ir(III)-based Agents for Monitoring Cytochrome P450 3A4 Active Site Occupancy

Madeline Denison,[†] Sean J. Steinke, [‡] Aliza Majeed,[⁂] Claudia Turro,[‡] Thomas A. Kocarek,[⁂] Irina F. Sevrioukova,[‖] and Jeremy J. Kodanko[†,§]

[†]*Department of Chemistry, Wayne State University, 5101 Cass Avenue, Detroit, Michigan 48202, United States*

[‡]*Department of Chemistry and Biochemistry, The Ohio State University, Columbus, Ohio 43210, United States*

[‖]*Molecular Biology and Biochemistry, University of California, Irvine, California 92697, United States*

[⁂]*Institute of Environmental Health Sciences, 6135 Woodward Avenue, Integrative Biosciences Center, Room 2126, Wayne State University, Detroit, MI 48202, United States*

[§]*Barbara Ann Karmanos Cancer Institute, Detroit, Michigan 48201, United States*

Supporting Information Placeholder

ABSTRACT: Cytochromes P450 (CYPs) are a superfamily of enzymes responsible for biosynthesis and drug metabolism. Monitoring the activity of CYP3A4, the major human drug-metabolizing enzyme, is vital for assessing metabolism of pharmaceuticals and identifying harmful drug-drug interactions. Existing probes for CYP3A4 are irreversible turn-on substrates that monitor activity at specific time points in end-point assays. To provide a more dynamic approach, we designed, synthesized and characterized emissive Ir(III) and Ru(II) complexes that allow monitoring of CYP3A4 active site occupancy in real time. In the bound state, probe emission is quenched by the active site heme. Upon displacement from the active site by CYP3A4-specific inhibitors or substrates, these probes show high emission turn-on. Direct probe binding to the CYP3A4 active site was confirmed by X-ray crystallography. The lead Ir(III)-based probe has nanomolar K_d and high selectivity for CYP3A4, efficient cellular uptake, and low toxicity in CYP3A4-overexpressing HepG2 cells.

Cytochromes P450 are crucial enzymes responsible for biomolecule synthesis and drug metabolism. Among 57 human CYPs, CYP3A4 is the major drug-metabolizing enzyme responsible for oxidizing the majority of pharmaceuticals.[1] Due to high substrate promiscuity and plasticity of the active site, CYP3A4 is implicated in many drug-drug interactions that can cause drug toxicity.[2–5] Additionally, CYP3A4 displays genetic polymorphism where mutations facilitate or slow down drug metabolism, thereby affecting therapeutic efficiency.[6–8] These attributes make CYP3A4 an important target for activity monitoring, especially in complex systems such as liver microsomes and hepatocytes that model human drug metabolism *in vitro*. Current methods for monitoring CYP3A4 activity involve marker substrates, which require cumbersome and costly HPLC analyses conducted over multiple time points, or irreversible turn-on reagents that make it difficult to monitor changes to CYP3A4 activity over time (Figure 1A).[9–14] As an alternative approach to these classical methods, in this communication we report emissive Ir(III) and Ru(II) complexes that allow sensing of occupancy of the CYP3A4 active site (Figure 1B).

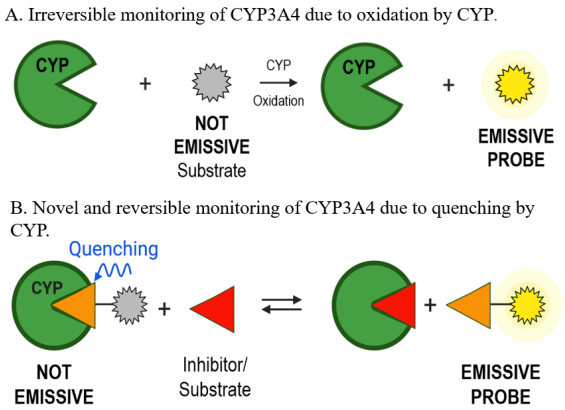

Figure 1. Emissive probes for monitoring metabolism by CYP3A4.

We chose to examine Ir(III) and Ru(II) complexes as probes for CYP3A4 because they are powerful tools for monitoring biological activity.[15–24] Probes of this class have long luminescence lifetimes, ranging from hundreds of nanoseconds up to ~100 µs,[15,16,25] which allows for time-resolved gating that can be used to exclude background emission from biomolecules and fluorogenic substrates.

Thus, these compounds were expected to provide a distinct advantage over previous CYP3A4 probes containing organic-based fluorescent groups,[26] whose low nanosecond lifetimes preclude the measurement of CYP activity in human liver microsomes, the gold standard in drug metabolism.

Transition metal-based probes were designed to interact with a hydrophobic surface within the substrate access channel of CYP3A4,[27] and included a pyridyl side chain (see R_1, Figure 2) to anchor the complex to the enzyme through direct heme iron coordination. Emissive sensors **2**–**5** were synthesized as racemic mixtures of Δ and Λ isomers (Figure 2A). Ligand **1** was heated with Ru(II) precursors *cis*-[Ru(L_1)$_2$Cl$_2$] (L_1 = 2,2'-bipyridine or 1,10-phenanthroline), which gave compounds **2** and **3**. Alternatively, treating **1** with [Ir(μ-Cl)(C^N)$_2$]$_2$ [C^N = 2-phenylpyridine (ppy) or 2-phenylquinoline (pq)] gave complexes **4** and **5**. Complexes **2**–**5** were characterized by ^{1}H NMR, IR and electronic absorption spectroscopies and electrospray mass spectrometry. All data were consistent with the structures shown in Figure 2. Importantly, electronic absorption and emission spectra for **2**–**5** were in good agreement with data for the parent Ru(II) or Ir(III) complexes devoid of the R_1 side chain.[28–30] All complexes emit brightly when excited with 435 nm light (Figure S7), with **4** having the highest emission quantum yield of 0.086(9) and a remarkable lifetime of 1.6 μs, over twice as long as **2** and **3** (Table 1).

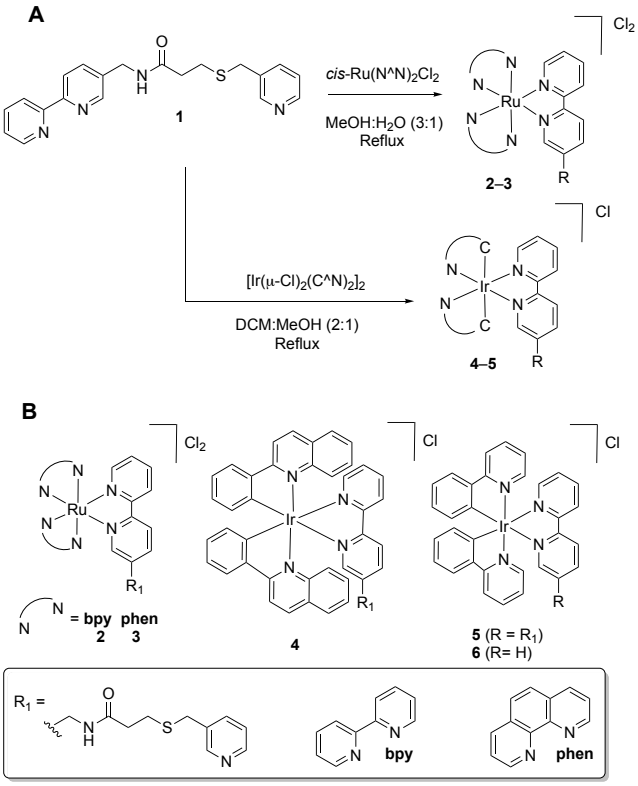

Figure 2. Synthesis (**A**) and structures (**B**) of Ir(III) and Ru(II) CYP3A4 photosensors **2**-**5**.

Equilibrium titration of CYP3A4 with **2**–**5** showed that all complexes exhibit type II binding, indicative of strong pyridine nitrogen coordination to the heme (Figures 3A, C-F). Spectral dissociation constants for **2**–**5** are listed in Table 1. Complexes **4** and **5** are far more potent than Ru(II) inhibitors **2** and **3,** indicating that CYP3A4 preferably binds monocationic over dicationic complexes. Importantly, attachment of the R_1 side chain dramatically increases the inhibitory potency, by nearly 100-fold. Control compound **6** shows type I binding (blue shift in the Soret band) and is a weak inhibitor with a K_d of 11.2 ± 0.08 μM, whereas analog **5** with the pyridyl containing R_1 chain exhibits type II binding, with a stronger affinity of 130 ± 11 nM. Both the binding affinity determined from the equilibrium titrations and the IC_{50} data indicated that Ir(III) sensors bind tighter and inhibit CYP3A4 more potently than Ru(II) compounds, with tunable K_d values as low as 70 ± 2 nM for **4**.

Table 1. Dissociation constants (K_d), IC_{50} values for CYP3A4 (μM) and emission quantum yields for sensors **2** – **5**.

Compound	K_d[a] (μM)	IC_{50}[b] (μM)	Φ_{em}[c] (H_2O)	τ/ μs (H_2O)
2	53±4	6.0±0.5	0.046(3)	0.66
3	23±2	3.1±0.4	0.042(9)	0.75
4	0.070±.0.002	0.25±0.02	0.086(9)	1.6
5	0.130±0.011	0.20±0.01	0.007(1)	0.062
6	11.2±0.8	1.02±0.02	ND	ND

[a]Determined by spectrophotometric titration assay. [b]CYP3A4 activity assay with BFC, 293 ± 3K, 0.2 μM CYP3A4, 0.3 μM cytochrome P450 reductase, vs. DMSO control (100% activity), standard error <10%. [c]Emission spectra of absorption matched solutions in argon sparged H_2O (A_{435} ~ 0.07), λ_{ex} = 435 nm, 455 nm longpass filter, referenced to Ru(bpy)$_3$ Φ_{em} = 0.042.

Next, Ir(III) complexes **4** and **5** were co-crystallized with CYP3A4 (Figure 3C-F, S8). In both structures, the inhibitor's R_1 side chain curls above the heme and the terminal pyridine nitrogen ligates to the heme iron (Fe-N distance of 2.20-2.23 Å). Hydrophobic residues Phe108, Phe220, Phe57, and Leu482 are in close contact with the ppy and pq groups of **4** and **5**, respectively. Electron density was well defined for the heme-ligating pyridine, part of the tether, and the Ir(III) cores. The Ir ligands were poorly defined, which suggests that both the Δ and Λ isomers of **4** and **5** were bound to the active site. Stereochemistry was not specified during structural refinement, but the Λ and Δ isomers (shown in Figure 3C-F) were preferably selected for **4** and **5**, respectively, and fit into electron density maps by the refining program. Importantly, **4** and **5** are the first iridium complexes characterized to bind to a CYP enzyme.[31–38]

To ensure that **4** binds to CYP3A4 more selectively than to other CYP isoforms, IC_{50}s of **4** against CYP3A4, CYP1A2, and CYP2C9 were determined using commercially available inhibitor screening kits (BioVision). Data from these kits vs. the soluble reconstituted system in Table 1 can not be compared directly because they were acquired under different conditions.[27] Derived IC_{50} values were 2.8 ± 1.0 μM, >100 μM and 79 ± 6 μM for CYP3A4, CYP2C9 and CYP1A2, respectively (Figure 3G). The 28- and >36-fold difference in IC_{50} demonstrates the high selectivity and preferential binding of **4** to a larger and expandable active site of CYP3A4 (Figure S8). For comparison, the volume of the active site cavity in ligand-free CYP3A4 is 1400 Å^3 as compared to 375 Å^3 and 470 Å^3 in CYP1A2 and CYP2C9, respectively.[7,39,40]

With compound **4** identified as a lead, we evaluated its ability to act as an active site photosensor by measuring changes in emission upon addition of ligand-free or substrate/inhibitor-bound CYP3A4 (Figure 3H). Strong luminescence quenching was observed when **4** (5 μM) was mixed with ligand-free CYP3A4 (3 μM), consistent with other emissive probes for P450 enzymes.[41–45] The quenching was partial when CYP3A4 was bound to a substrate or inhibitor prior to addition of **4**. Importantly, the emission levels were ligand dependent and correlated with the ligands' binding

affinity: the strongest CYP3A4 binder, ritonavir (K_d = 19 nM), was the most difficult to displace, whereas the weakly bound substrate, testosterone (K_d of 1.5 μM and 30 μM for two binding sites), was expelled by the probe more easily.

recovers in a manner proportional to the binding affinity of CYP3A4 substrates and inhibitors. Furthermore, photosensor **4** penetrates and inhibits CYP3A4 in hepatic cells, and emits brightly in the intracellular environment. This new class of photosensors is

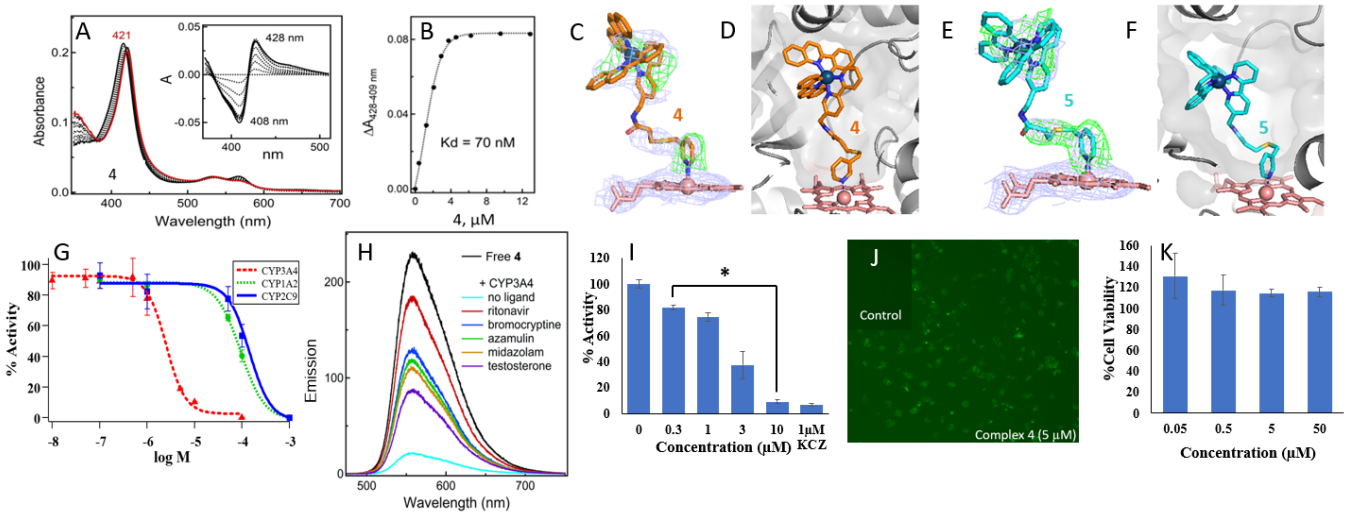

Figure 3. (A) Spectral changes observed during equilibrium titration of CYP3A4 with **4**, inset is difference spectra; (B) Titration plot with derived K_d value; (C, D) Crystal structure of the **4**-CYP3A4 complex at 2.78 Å resolution (PDB ID 7UAY). (E, F) Crystal structure of the **5**-CYP3A4 complex at 2.65 Å resolution (PDB ID 7UAZ). Blue and green mesh in panels H and J are $2F_o$-F_c and polder omit electron density maps contoured at 1σ and 3σ levels, respectively; (G) Inhibition of CYP3A4, CYP1A4, CYP2C9 activity by **4**; (H) Fluorescence spectra of **4** (5 μM) in the absence and presence of CYP3A4 (3 μM) bound to different substrates and inhibitors (10–20 μM) showing ligand-dependent emission yields (0.1 M PBS, pH 7.4, 10% glycerol, λ_{ex} = 433 nm); (I) CYP3A4 activity with **4** (0.3–10 μM) determined by P450-Glo CYP3A4 Assay or ketoconazole (1 μM) as positive control; Concentrations 0.3 – 10 μM are statistically significant from control containing vehicle; *P < 0.05; (J) Fluorescence microscopy images (GFP filter) of HepG2-CYP3A4 cells treated with **4** (5 μM), (J) Inset is control fluorescence from vehicle treated cells; (K) Cell viability at different concentrations of **4** (0.05–50 μM) determined by a cellular viability assay (MTT, 72 h).

To further substantiate the scope of our lead compound **4**, we assessed its inhibitory properties in HepG2 human hepatoma cells, where expression of most drug-metabolizing CYPs is negligible or absent. However, when HepG2 cells are stably engineered with vectors expressing CYPs, protein levels reach those in primary human hepatocytes, which makes this model cell line a convenient *in vitro* tool to mimic drug metabolism in the liver.[46–48] To determine the CYP3A4 inhibitory activity of **4**, HepG2 cells overexpressing CYP3A4 were used in conjuction with a bioluminiscent P450-Glo CYP3A4 assay. Importantly, a strong concentration-dependent decrease in activity was observed, with statistically significant inhibition at 300 nM (Figure 3I, ~20% inhibition, P < 0.05 vs control). These data confirm that **4** is able to efficiently penetrate HepG2-CYP3A4 cells and inhibit CYP3A4 activity at nanomolar concentrations.

Finally, to demonstrate that our photosensors can be visualized in cells, we employed fluorescence microscopy. HepG2-CYP3A4 cells were treated with **4** (5 μM) for 1 h (Figure 3J), then rinsed with PBS (pH 7.0) and imaged using the GFP channel. We found that **4** is cell-permeable and can be visually detected at concentrations as low as 5 μM. Utilization of metal complexes at such low concentrations limits their cell toxicity. In fact, **4** is well tolerated by HepG2-CYP3A4 cells (EC_{50} > 50 μM), as judged by a cellular viability assay (Figure 3K, MTT, 72 h). This result provides strong evidence that cell toxicity can be avoided or largely minimized when Ir(III) complexes are used as photosensors at low concentrations (<10 μM).

In summary, Ir(III) compound **4** is a potent and specific inhibitor that serves as a photosensor for CYP3A4 active site occupancy. The luminescence of **4** is quenched upon binding to CYP3A4 and expected to provide a significant advantage over traditional endpoint assays currently used for detection of drug-drug interactions of CYP3A4 in cells. Another beneficial property of our photosensors is their prolonged luminescence lifetimes, which allows time-resolved fluorescence measurements for excluding autofluorescence, a major problem in bio-imaging that cannot be addressed with current sensors. Studies are now underway in our laboratories to further develop this class of compounds and utilize Ir(III) photosensors for monitoring CYP3A4 active site occupancy *in cellulo*.

ASSOCIATED CONTENT

Supporting Information

The Supporting Information is available free of charge on the ACS Publications website.

Experimental procedures for synthesis and spectral data for **2**–**5**, procedures for photophysical, pharmacological and biological studies, X-ray crystallographic data

AUTHOR INFORMATION

Corresponding Author

Claudia Turro – Department of Chemistry and Biochemistry, The Ohio State University, Columbus, Ohio 43210, United States; orcid.org/0000-0003-3202-5870; Email: turro@chemistry.ohio-state.edu

Irina F. Sevrioukova – Molecular Biology and Biochemistry, University of California, Irvine, California 92697, United States; orcid.org/0000-0002-4498-6057; Email: sevrioui@uci.edu

Thomas A. Kocarek – Institute of Environmental Health Sciences, 6135 Woodward Avenue, Integrative Biosciences Center, Room 2126, Wayne State University, Detroit, MI 48202, United States. E-mail: t.kocarek@wayne.edu.
Jeremy J. Kodanko − Department of Chemistry, Wayne State University, Detroit, Michigan 48202, United States; Barbara Ann Karmanos Cancer Institute, Detroit, Michigan 48201, United States; orcid.org/0000-0001-5196-7463; Email: jkodanko@chem.wayne.edu

Author Contributions

Madeline Denison - Department of Chemistry, Wayne State University, Detroit, Michigan 48202, United States; orcid.org/0000-0002-6272-6283.
Sean J. Steinke - Department of Chemistry and Biochemistry, The Ohio State University, Columbus, Ohio 43210, United States.
Aliza Majeed - Institute of Environmental Health Sciences, 6135 Woodward Avenue, Integrative Biosciences Center, Room 2126, Wayne State University, Detroit, MI 48202

Notes

The authors declare no competing financial interests.

ACKNOWLEDGMENT

We gratefully acknowledge the National Science Foundation (CHE 1800395, CHE 1764235), the National Institutes of Health (ES025767 and T32GM142519), Richard Barber Interdisciplinary Research Program, and Wayne State University for support of this research. We thank Dr. Lei Guo of the National Center for Toxicology Research for generously providing HepG2-CYP3A4 cells. This research was carried out at the Stanford Synchrotron Radiation Lightsource (SSRL) beamline 12-2. The SLAC National Accelerator Laboratory is supported by the U.S. Department of Energy (DE-AC02-76SF00515). SSRL Structural Molecular Biology Program is supported by the Department of Energy and National Institutes of Health (P30GM133894).

REFERENCES

(1) Hodgson, E. In Vitro Human Phase I Metabolism of Xenobiotics I: Pesticides and Related Compounds Used in Agriculture and Public Health, May 2003. *J. Biochem. Mol. Toxicol.* **2003**, *17* (4), 201–206. https://doi.org/10.1002/jbt.10080.

(2) Chapman, S. A.; Lake, K. D. Considerations for Using Ketoconazole in Solid Organ Transplant Recipients Receiving Cyclosporine Immunosuppression. *J. Transpl. Coord.* **1996**, *6* (3), 7.

(3) van Eijk, M.; Boosman, R. J.; Schinkel, A. H.; Huitema, A. D. R.; Beijnen, J. H. Cytochrome P450 3A4, 3A5, and 2C8 Expression in Breast, Prostate, Lung, Endometrial, and Ovarian Tumors: Relevance for Resistance to Taxanes. *Cancer Chemother. Pharmacol.* **2019**, *84* (3), 487–499. https://doi.org/10.1007/s00280-019-03905-3.

(4) Brayer, S. W.; Reddy, K. R. Ritonavir-Boosted Protease Inhibitor Based Therapy: A New Strategy in Chronic Hepatitis C Therapy. *Expert Rev. Gastroenterol. Hepatol.* **2015**, *9* (5), 547–558. https://doi.org/10.1586/17474124.2015.1032938.

(5) Kempf, D. J.; Marsh, K. C.; Kumar, G.; Rodrigues, A. D.; Denissen, J. F.; McDonald, E.; Kukulka, M. J.; Hsu, A.; Granneman, G. R.; Baroldi, P. A.; Sun, E.; Pizzuti, D.; Plattner, J. J.; Norbeck, D. W.; Leonard, J. M. Pharmacokinetic Enhancement of Inhibitors of the Human Immunodeficiency Virus Protease by Coadministration with Ritonavir. *Antimicrob. Agents Chemother.* **1997**, *41* (3), 654–660. https://doi.org/10.1128/AAC.41.3.654.

(6) Lynch, T.; Price, A. The Effect of Cytochrome P450 Metabolism on Drug Response, Interactions, and Adverse Effects. *Cytochrome P* **2007**, *76* (3), 6.

(7) Zanger, U. M.; Schwab, M. Cytochrome P450 Enzymes in Drug Metabolism: Regulation of Gene Expression, Enzyme Activities, and Impact of Genetic Variation. *Pharmacol. Ther.* **2013**, *138* (1), 103–141. https://doi.org/10.1016/j.pharmthera.2012.12.007.

(8) Johansson, I.; Ingelman-Sundberg, M. Genetic Polymorphism and Toxicology—With Emphasis on Cytochrome P450. *Toxicol. Sci.* **2011**, *120* (1), 1–13. https://doi.org/10.1093/toxsci/kfq374.

(9) Sevrioukova, I. F.; Poulos, T. L. Current Approaches for Investigating and Predicting Cytochrome P450 3A4-Ligand Interactions. In *Monooxygenase, Peroxidase and Peroxygenase Properties and Mechanisms of Cytochrome P450*; Hrycay, E. G., Bandiera, S. M., Eds.; Advances in Experimental Medicine and Biology; Springer International Publishing: Cham, 2015; Vol. 851, pp 83–105. https://doi.org/10.1007/978-3-319-16009-2_3.

(10) Raunio, H.; Pentikäinen, O.; Juvonen, R. O. Coumarin-Based Profluorescent and Fluorescent Substrates for Determining Xenobiotic-Metabolizing Enzyme Activities In Vitro. *Int. J. Mol. Sci.* **2020**, *21* (13), 4708. https://doi.org/10.3390/ijms21134708.

(11) Ning, J.; Liu, T.; Dong, P.; Wang, W.; Ge, G.; Wang, B.; Yu, Z.; Shi, L.; Tian, X.; Huo, X.; Feng, L.; Wang, C.; Sun, C.; Cui, J.; James, T. D.; Ma, X. Molecular Design Strategy to Construct the Near-Infrared Fluorescent Probe for Selectively Sensing Human Cytochrome P450 2J2. *J. Am. Chem. Soc.* **2019**, *141* (2), 1126–1134. https://doi.org/10.1021/jacs.8b12136.

(12) Dai, Z.-R.; Ge, G.-B.; Feng, L.; Ning, J.; Hu, L.-H.; Jin, Q.; Wang, D.-D.; Lv, X.; Dou, T.-Y.; Cui, J.-N.; Yang, L. A Highly Selective Ratiometric Two-Photon Fluorescent Probe for Human Cytochrome P450 1A. *J. Am. Chem. Soc.* **2015**, *137* (45), 14488–14495. https://doi.org/10.1021/jacs.5b09854.

(13) Ning, J.; Tian, Z.; Wang, B.; Ge, G.; An, Y.; Hou, J.; Wang, C.; Zhao, X.; Li, Y.; Tian, X.; Yu, Z.; Huo, X.; Sun, C.; Feng, L.; Cui, J.; Ma, X. A Highly Sensitive and Selective Two-Photon Fluorescent Probe for Real-Time Sensing of Cytochrome P450 1A1 in Living Systems. *Mater. Chem. Front.* **2018**, *2* (11), 2013–2020. https://doi.org/10.1039/C8QM00372F.

(14) Dai, Z.-R.; Feng, L.; Jin, Q.; Cheng, H.; Li, Y.; Ning, J.; Yu, Y.; Ge, G.-B.; Cui, J.-N.; Yang, L. A Practical Strategy to Design and Develop an Isoform-Specific Fluorescent Probe for a Target Enzyme: CYP1A1 as a Case Study. *Chem. Sci.* **2017**, *8* (4), 2795–2803. https://doi.org/10.1039/C6SC03970G.

(15) Martí, A. A. Metal Complexes and Time-Resolved Photoluminescence Spectroscopy for Sensing Applications. *J. Photochem. Photobiol. Chem.* **2015**, *307–308*, 35–47. https://doi.org/10.1016/j.jphotochem.2015.03.020.

(16) Huang, K.; Jiang, C.; Martí, A. A. Ascertaining Free Histidine from Mixtures with Histidine-Containing Proteins Using Time-Resolved Photoluminescence Spectroscopy. *J. Phys. Chem. A* **2014**, *118* (45), 10353–10358. https://doi.org/10.1021/jp502837a.

(17) Lampe, J. N.; Atkins, W. M. Time-Resolved Fluorescence Studies of Heterotropic Ligand Binding to Cytochrome P450 3A4 †. *Biochemistry* **2006**, *45* (40), 12204–12215. https://doi.org/10.1021/bi060083h.

(18) Sreedharan, S.; Sinopoli, A.; Jarman, Paul. J.; Robinson, D.; Clemmet, C.; Scattergood, P. A.; Rice, C. R.; Smythe, Carl. G. W.; Thomas, J. A.; Elliott, P. I. P. Mitochondria-Localising DNA-Binding Biscyclometalated Phenyltriazole Iridium(III) Dipyridophenazene Complexes: Syntheses and Cellular Imaging Properties. *Dalton Trans.* **2018**, *47* (14), 4931–4940. https://doi.org/10.1039/C8DT00046H.

(19) Liu, H.-W.; Law, W. H.-T.; Lee, L. C.-C.; Lau, J. C.-W.; Lo, K. K.-W. Cyclometalated Iridium(III) Bipyridine-Phenylboronic Acid Complexes as Bioimaging Reagents and Luminescent Probes for Sialic Acids. *Chem. - Asian J.* **2017**, *12* (13), 1545–1556. https://doi.org/10.1002/asia.201700359.

(20) Wang, W.; Lu, L.; Wu, K.-J.; Liu, J.; Leung, C.-H.; Wong, C.-Y.; Ma, D.-L. Long-Lived Iridium(III) Complexes as Luminescent Probes for the Detection of Periodate in Living Cells. *Sens. Actuators B Chem.* **2019**, *288*, 392–398. https://doi.org/10.1016/j.snb.2019.03.019.

(21) Zhang, C.; Qiu, K.; Liu, C.; Huang, H.; Rees, T. W.; Ji, L.; Zhang, Q.; Chao, H. Tracking Mitochondrial Dynamics during Apoptosis with Phosphorescent Fluorinated Iridium(III) Complexes. *Dalton*

Trans. **2018**, *47* (37), 12907–12913. https://doi.org/10.1039/C8DT02918K.

(22) Wu, X.; Zheng, Y.; Wang, F.; Cao, J.; Zhang, H.; Zhang, D.; Tan, C.; Ji, L.; Mao, Z. Anticancer Ir ^{III} –Aspirin Conjugates for Enhanced Metabolic Immuno-Modulation and Mitochondrial Lifetime Imaging. *Chem. – Eur. J.* **2019**, *25* (28), 7012–7022. https://doi.org/10.1002/chem.201900851.

(23) Shaikh, S.; Wang, Y.; ur Rehman, F.; Jiang, H.; Wang, X. Phosphorescent Ir (III) Complexes as Cellular Staining Agents for Biomedical Molecular Imaging. *Coord. Chem. Rev.* **2020**, *416*, 213344. https://doi.org/10.1016/j.ccr.2020.213344.

(24) Cook, N. P.; Torres, V.; Jain, D.; Martí, A. A. Sensing Amyloid-β Aggregation Using Luminescent Dipyridophenazine Ruthenium(II) Complexes. *J. Am. Chem. Soc.* **2011**, *133* (29), 11121–11123. https://doi.org/10.1021/ja204656r.

(25) Huang, K.; Bulik, I. W.; Martí, A. A. Time-Resolved Photoluminescence Spectroscopy for the Detection of Cysteine and Other Thiol Containing Amino Acids in Complex Strongly Autofluorescent Media. *Chem. Commun.* **2012**, *48* (96), 11760. https://doi.org/10.1039/c2cc36588j.

(26) Chougnet, A.; Grinkova, Y.; Ricard, D.; Sligar, S.; Woggon, W.-D. Fluorescent Probes for Rapid Screening of Potential Drug–Drug Interactions at the CYP3A4 Level. *ChemMedChem* **2007**, *2* (5), 717–724. https://doi.org/10.1002/cmdc.200600300.

(27) Toupin, N.; Steinke, S. J.; Nadella, S.; Li, A.; Rohrabaugh, T. N.; Samuels, E. R.; Turro, C.; Sevrioukova, I. F.; Kodanko, J. J. Photosensitive Ru(II) Complexes as Inhibitors of the Major Human Drug Metabolizing Enzyme CYP3A4. *J. Am. Chem. Soc.* **2021**, *143* (24), 9191–9205. https://doi.org/10.1021/jacs.1c04155.

(28) Kwon, T.-H.; Oh, Y. H.; Shin, I.-S.; Hong, J.-I. New Approach Toward Fast Response Light-Emitting Electrochemical Cells Based on Neutral Iridium Complexes via Cation Transport. *Adv. Funct. Mater.* **2009**, *19* (5), 711–717. https://doi.org/10.1002/adfm.200801231.

(29) Wu, S.-H.; Ling, J.-W.; Lai, S.-H.; Huang, M.-J.; Cheng, C. H.; Chen, I.-C. Dynamics of the Excited States of $[Ir(Ppy)_2 Bpy]^+$ with Triple Phosphorescence. *J. Phys. Chem. A* **2010**, *114* (38), 10339–10344. https://doi.org/10.1021/jp102264q.

(30) Bouskila, A.; Drahi, B.; Amouyal, E.; Sasaki, I.; Gaudemer, A. Mononuclear and Binuclear Ruthenium(II) Heteroleptic Complexes Based on 1,10-Phenanthroline Ligands. *J. Photochem. Photobiol. Chem.* **2004**, *163* (3), 381–388. https://doi.org/10.1016/j.jphotochem.2004.01.007.

(31) Wu, S.; Zhou, Y.; Rebelein, J. G.; Kuhn, M.; Mallin, H.; Zhao, J.; Igareta, N. V.; Ward, T. R. Breaking Symmetry: Engineering Single-Chain Dimeric Streptavidin as Host for Artificial Metalloenzymes. *J. Am. Chem. Soc.* **2019**, *141* (40), 15869–15878. https://doi.org/10.1021/jacs.9b06923.

(32) Feng, L.; Geisselbrecht, Y.; Blanck, S.; Wilbuer, A.; Atilla-Gokcumen, G. E.; Filippakopoulos, P.; Kräling, K.; Celik, M. A.; Harms, K.; Maksimoska, J.; Marmorstein, R.; Frenking, G.; Knapp, S.; Essen, L.-O.; Meggers, E. Structurally Sophisticated Octahedral Metal Complexes as Highly Selective Protein Kinase Inhibitors. *J. Am. Chem. Soc.* **2011**, *133* (15), 5976–5986. https://doi.org/10.1021/ja1112996.

(33) Rebelein, J. G.; Cotelle, Y.; Garabedian, B.; Ward, T. R. Chemical Optimization of Whole-Cell Transfer Hydrogenation Using Carbonic Anhydrase as Host Protein. *ACS Catal.* **2019**, *9* (5), 4173–4178. https://doi.org/10.1021/acscatal.9b01006.

(34) Monnard, F. W.; Nogueira, E. S.; Heinisch, T.; Schirmer, T.; Ward, T. R. Human Carbonic Anhydrase II as Host Protein for the Creation of Artificial Metalloenzymes: The Asymmetric Transfer Hydrogenation of Imines. *Chem. Sci.* **2013**, *4* (8), 3269. https://doi.org/10.1039/c3sc51065d.

(35) Sullivan, M. P.; Cziferszky, M.; Tolbatov, I.; Truong, D.; Mercadante, D.; Re, N.; Gust, R.; Goldstone, D. C.; Hartinger, C. G. Probing the Paradigm of Promiscuity for N-Heterocyclic Carbene Complexes and Their Protein Adduct Formation. *Angew. Chem. Int. Ed.* **2021**, *60* (36), 19928–19932. https://doi.org/10.1002/anie.202106906.

(36) Robles, V. M.; Dürrenberger, M.; Heinisch, T.; Lledós, A.; Schirmer, T.; Ward, T. R.; Maréchal, J.-D. Structural, Kinetic, and Docking Studies of Artificial Imine Reductases Based on Biotin–Streptavidin Technology: An Induced Lock-and-Key Hypothesis. *J. Am. Chem. Soc.* **2014**, *136* (44), 15676–15683. https://doi.org/10.1021/ja508258t.

(37) Heinisch, T.; Pellizzoni, M.; Dürrenberger, M.; Tinberg, C. E.; Köhler, V.; Klehr, J.; Häussinger, D.; Baker, D.; Ward, T. R. Improving the Catalytic Performance of an Artificial Metalloenzyme by Computational Design. *J. Am. Chem. Soc.* **2015**, *137* (32), 10414–10419. https://doi.org/10.1021/jacs.5b06622.

(38) Stein, A.; Chen, D.; Igareta, N. V.; Cotelle, Y.; Rebelein, J. G.; Ward, T. R. A Dual Anchoring Strategy for the Directed Evolution of Improved Artificial Transfer Hydrogenases Based on Carbonic Anhydrase. *ACS Cent. Sci.* **2021**, *7* (11), 1874–1884. https://doi.org/10.1021/acscentsci.1c00825.

(39) Yano, J. K.; Wester, M. R.; Schoch, G. A.; Griffin, K. J.; Stout, C. D.; Johnson, E. F. The Structure of Human Microsomal Cytochrome P450 3A4 Determined by X-Ray Crystallography to 2.05-Å Resolution. *J. Biol. Chem.* **2004**, *279* (37), 38091–38094. https://doi.org/10.1074/jbc.C400293200.

(40) Williams, P. A.; Cosme, J.; Ward, A.; Angove, H. C.; Matak Vinković, D.; Jhoti, H. Crystal Structure of Human Cytochrome P450 2C9 with Bound Warfarin. *Nature* **2003**, *424* (6947), 464–468. https://doi.org/10.1038/nature01862.

(41) Hays, A.-M. A.; Dunn, A. R.; Chiu, R.; Gray, H. B.; Stout, C. D.; Goodin, D. B. Conformational States of Cytochrome P450cam Revealed by Trapping of Synthetic Molecular Wires. *J. Mol. Biol.* **2004**, *344* (2), 455–469. https://doi.org/10.1016/j.jmb.2004.09.046.

(42) Dunn, A. R.; Hays, A.-M. A.; Goodin, D. B.; Stout, C. D.; Chiu, R.; Winkler, J. R.; Gray, H. B. Fluorescent Probes for Cytochrome P450 Structural Characterization and Inhibitor Screening. 2.

(43) Dmochowski, I. J.; Crane, B. R.; Wilker, J. J.; Winkler, J. R.; Gray, H. B. Optical Detection of Cytochrome P450 by Sensitizer-Linked Substrates. 4.

(44) Dunn, A. R.; Dmochowski, I. J.; Bilwes, A. M.; Gray, H. B.; Crane, B. R. Probing the Open State of Cytochrome P450cam with Ruthenium-Linker Substrates. *Proc. Natl. Acad. Sci.* **2001**, *98* (22), 12420–12425. https://doi.org/10.1073/pnas.221297998.

(45) Contakes, S. M.; Juda, G. A.; Langley, D. B.; Halpern-Manners, N. W.; Duff, A. P.; Dunn, A. R.; Gray, H. B.; Dooley, D. M.; Guss, J. M.; Freeman, H. C. Reversible Inhibition of Copper Amine Oxidase Activity by Channel-Blocking Ruthenium(II) and Rhenium(I) Molecular Wires. 6.

(46) Chen, S.; Wu, Q.; Li, X.; Li, D.; Mei, N.; Ning, B.; Puig, M.; Ren, Z.; Tolleson, W. H.; Guo, L. Characterization of Cytochrome P450s (CYP)-Overexpressing HepG2 Cells for Assessing Drug and Chemical-Induced Liver Toxicity. *J. Environ. Sci. Health Part C* **2021**, *39* (1), 68–86. https://doi.org/10.1080/26896583.2021.1880242.

(47) Xuan, J.; Chen, S.; Ning, B.; Tolleson, W. H.; Guo, L. Development of HepG2-Derived Cells Expressing Cytochrome P450s for Assessing Metabolism-Associated Drug-Induced Liver Toxicity. *Chem. Biol. Interact.* **2016**, *255*, 63–73. https://doi.org/10.1016/j.cbi.2015.10.009.

(48) Yoshitomi, S.; Ikemoto, K.; Takahashi, J.; Miki, H.; Namba, M.; Asahi, S. Establishment of the Transformants Expressing Human Cytochrome P450 Subtypes in HepG2, and Their Applications on Drug Metabolism and Toxicology. *Toxicol. In Vitro* **2001**, *15* (3), 245–256. https://doi.org/10.1016/S0887-2333(01)00011-X.

TOC Graphic

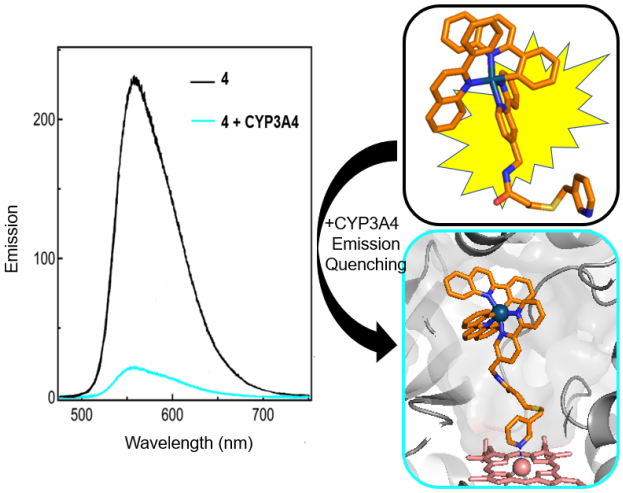

TOC Synopsis: Potent and selective Ir(III)-based CYP3A4 inhibitors were designed and synthesized to act as chemical tools for probing CYP3A4 active site occupancy. Importantly, our Ir(III) probes are highly emissive and have long emission lifetimes. Emission of Ir(III) becomes quenched in the CYP3A4 active site and addition of substrate or inhibitors of CYP3A4 results in emission turn-on.